

Synthesis, solvatochromism, and biological activity of novel azo dyes bearing 2-pyridone and benzimidazole moieties

Dušan MIJIN^{1,*}, Biljana BOŽIĆ NEDELJKOVIĆ², Bojan BOŽIĆ², Ilijana KOVRLIJA¹,
Jelena LAĐAREVIĆ¹, Gordana UŠĆUMLIĆ¹

¹Faculty of Technology and Metallurgy, University of Belgrade, Belgrade, Serbia

²Institute of Physiology and Biochemistry, Faculty of Biology, University of Belgrade, Belgrade, Serbia

Received: 30.11.2017

Accepted/Published Online: 02.04.2018

Final Version: 01.06.2018

Abstract: New azo dyes bearing 2-pyridone and benzimidazole moieties were prepared using diazotization of 4-(1H-benzo[d]imidazol-2-yl)aniline and coupling of the obtained diazonium salt with substituted 3-cyano-2-pyridones. Obtained compounds were characterized via UV-Vis, FT-IR, and ¹H and ¹³C NMR spectroscopy as well as by elemental analysis data. The UV-Vis spectra of the synthesized dyes were measured in thirteen solvents of different properties at room temperature. Solvatochromism and tautomerism of novel azo dyes were discussed. An MTT (3,4,5-dimethylthiazol-2-yl)-2,5-diphenyl tetrazolium bromide) test was performed to prove the biocompatibility of the investigated dyes. The investigated dyes exhibited satisfying antiproliferative activities against both tumor cell lines, MDA-MB-231 and HCT-116, demonstrating the potent capacity for treatment of tumors.

Key words: UV-Vis spectroscopy, azo dyes, biocompatibility, antiproliferative activity, tautomerism

1. Introduction

Heterocyclic compounds can be found in many natural and synthetic compounds. They have a wide range of applications, mostly in pharmaceuticals, as well as in color chemistry. Among these compounds, benzimidazole and 2-pyridone have gained wide interest due to their biological, clinical, and industrial applications.

Benzimidazole in natural organic compounds is present as *N*-ribosyl-dimethylbenzimidazole and it can be found in vitamin B12 as an axial ligand for cobalt¹ as well as in DNA and RNA molecules.² Various benzimidazole derivatives exhibit different pharmacological activities such as antihypertensive,³ antiviral,⁴ antiulcer,⁵ antifungal,⁶ antibacterial,⁷ anticancer,⁸ and antihistaminic.⁹ The pharmaceutical activities of this class of compounds have been the subject of numerous review papers^{10–16} in which the structures of compounds were discussed along with their activity.

The 2-pyridone structure (dominant tautomer in pyridinol-pyridone tautomerism of 2-hydroxypyridine) is also present in DNA and RNA molecules.² 2-Pyridone derivatives possess pharmacological and a wide range of therapeutic activities.¹⁷ They exhibit antimicrobial,¹⁸ antiviral,¹⁹ anti-HIV,²⁰ anticancer,²¹ cardiotoxic,²² and vasorelaxant activities.²³ Pharmaceutically active derivatives obtained by a combination of benzimidazole and antimicrobial active 2-pyridone rings have also been synthesized and their potential biological applications have been observed.²⁴

*Correspondence: kavur@tmf.bg.ac.rs

Azo dyes represent the largest group of colored organic compounds due to the number of variations in the chemical structure and their wide commercial applications.^{25,26} They can be used for the dyeing of natural and synthetic fibers and for coloring plastics, rubber, foods, paints, varnishes, printing inks, drugs, and cosmetics. A number of dyes contain different heterocyclic moieties including benzimidazole and 2-pyridone cores. Benzimidazole-based dyes are used for dyeing of polyester²⁷ and polyamide fibers.²⁸ On the other hand, pyridone azo dyes are more abundant. These dyes are used as disperse dyes that are characterized by low aqueous solubility. Disperse dyes are usually applied to hydrophobic fibers like polyester and nylon. Some of the pyridone azo dyes are commercial products.²⁹ A synthesis of azo dyes containing benzimidazole and a 2-pyridone ring from 4-(4-methoxyphenyl)glutaconic anhydride was also reported.³⁰

In this work, we have prepared two dyes from 4-(1*H*-benzo[d]imidazol-2-yl)aniline and two 3-cyano-6-hydroxy-2-pyridones having different substituents in position 4 (methyl and phenyl) using a diazo-coupling reaction in order to examine the solvatochromic behavior in various solvents. The tautomerism of the synthesized dyes was also investigated. In addition, a study of the biological activities of the synthesized compounds was performed.

2. Results and discussion

The aryl azo pyridone dyes studied in this work were prepared according to the synthetic route given in Figure 1. The synthesis started with the preparation of 4-(1*H*-benzo[d]imidazol-2-yl)aniline (**1**) from *o*-phenylenediamine and *p*-aminobenzoic acid^{31,32} and continued with the diazotization of **1**. The prepared diazonium salt was then coupled with prepared pyridones,^{33,34} using a well-known procedure.³⁵ The structures of new compounds were characterized via UV-Vis, FT-IR, and ¹H and ¹³C NMR spectroscopy as well as elemental analysis data.

The analysis of FT-IR spectra of compounds **3a** and **3b** suggests the existence of a hydrazone form in the solid state. The conclusion was made due to the detection of two intense carbonyl bands (1619–1655 cm⁻¹) and a broad band ascribed to the N–H proton (3424–3426 cm⁻¹).

The NMR data obtained for compounds **3a** and **3b** at ambient temperature in DMSO-*d*₆ are given in Section 3. According to the analysis of NMR spectra the obtained dyes exist as hydrazone tautomers in DMSO-*d*₆. This was concluded by ¹H NMR shifts assigned to the imino proton of the hydrazone group, which are in the range of 14.55–14.71 ppm. This is in accordance with the literature data of the aryl azo pyridone dyes.^{33,34} The existence of the hydrazone form was further confirmed by the signals of two carbonyl groups in ¹³C NMR spectra observed in the range of 160.7–161.9 ppm.

2.1. Solvatochromism

The UV-Vis spectra of the synthesized dyes were measured in the range of 300–600 nm in thirteen solvents of different properties at room temperature (Table 1). Aryl azo pyridone dyes were characterized by azo-hydrazone tautomerism due to the proton exchange between a hydroxy group in the pyridone moiety and an azo group.²⁹ Possible tautomeric forms of the investigated dyes are given in Figure 2. Structure I is the azo form while Structure II represents the hydrazone form of the investigated dyes. The addition of a base leads to deprotonation and an anion is formed (Structure III). The formed anion is a resonance hybrid of two canonical structures: hydrazone (IIIa) and azo (IIIb).^{36–38} According to the data given in Table 1 and the UV-Vis spectra in Figures 3 and 4, the studied pyridone azo dyes exist generally in the hydrazone form, in the range of 438–457 nm for **3a** and 434–468 nm for **3b**, except in dipolar proton-accepting solvents (DMF, DMSO; Figure 4) where

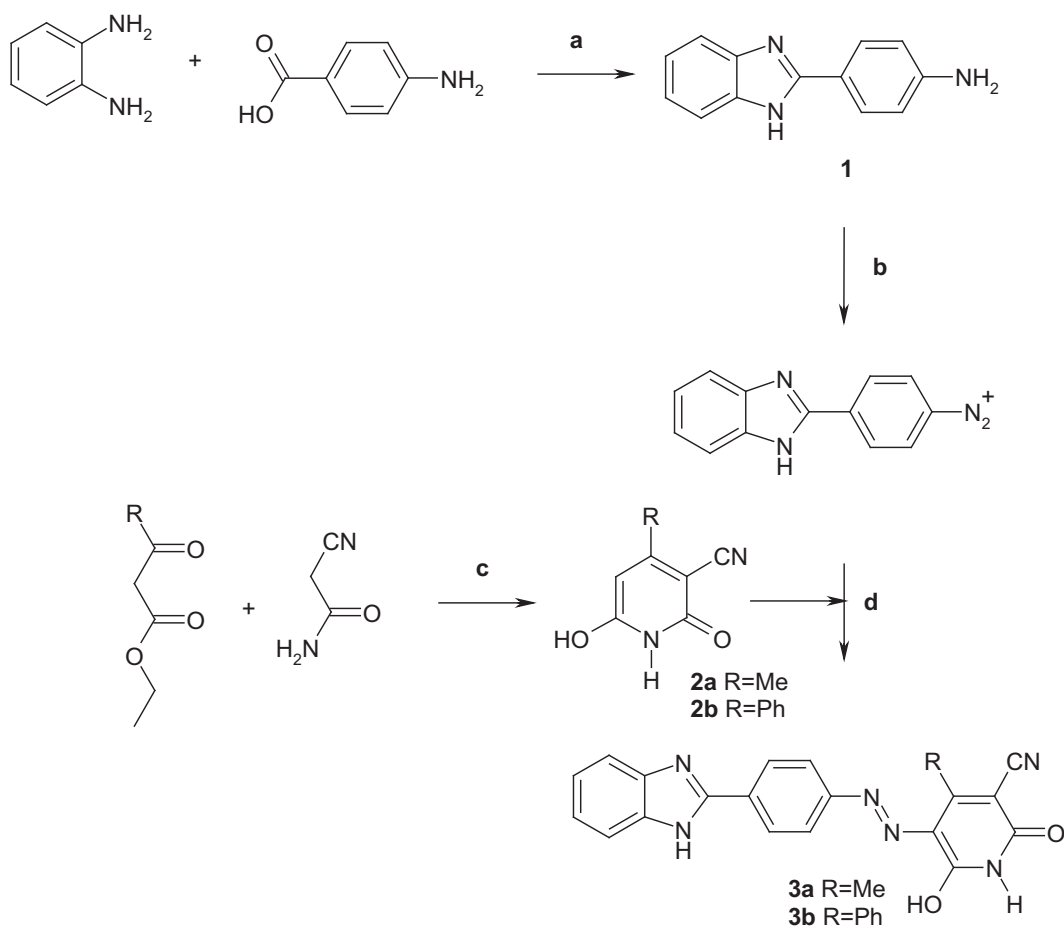


Figure 1. Reagents and conditions: a) H_3PO_3 / 180–200 °C; b) NaNO_2 , HCl / 0–5 °C; c) KOH , alcohol / reflux, d) KOH / 0–5 °C.

the hydrazone-anion equilibrium has been observed. The introduction of a phenyl group in position 4 of the pyridone moiety causes a bathochromic shift in comparison to a dye with a methyl group in same position. The bathochromic shift is small due to the spatial orientation of the phenyl group to the pyridone moiety and the absence of planarity.³⁹ Solvent polarity, on the other hand, has an almost negligible impact on the absorption maxima of the investigated dyes, but a slightly hypsochromic effect, with increase of polarity, can be observed. Moreover, a moderate bathochromic effect from ampholytic to aprotic solvents is also observed. Also, in solvents acting as a proton donors, such as acetic acid, a hypsochromic shift is observed with respect to proton-acceptor solvents (DMF, DMSO).

It is well known that the structure of the dye influences the acid-base equilibrium^{36–38} as presented in Figure 2 as well as the relative positions of UV-Vis maxima of hydrazone and anionic forms. In dipolar proton-accepting solvents aryl azo pyridone dyes can easily dissociate and an anion form can appear, as shown in Figures 3 and 4. The same can be achieved by the addition of a base. On the other hand, in acetic acid (proton-donating solvents) the hydrazone form is favorable (Figure 3). This can be achieved also by the addition of an acid. Thus, the concentrated hydrochloric acid and potassium hydroxide solution (1%) were added in drops to an ethanol solution of dyes in order to observe the position of hydrazone and anion forms. The UV-Vis

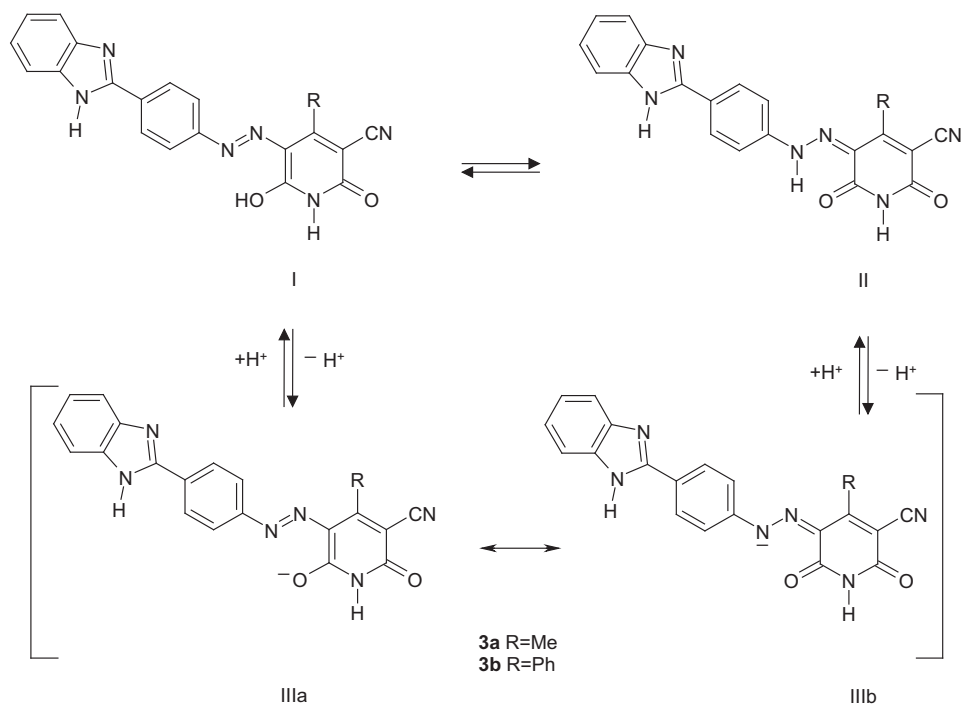


Figure 2. Possible tautomeric forms of the investigated aryl azo pyridone dyes.

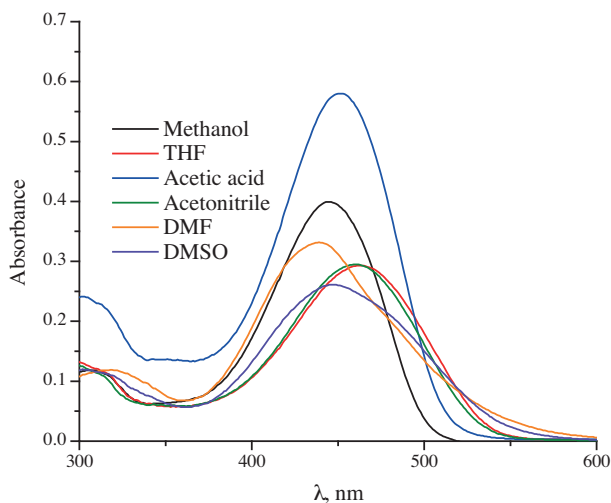


Figure 3. UV-Vis spectra of **3b** in selected solvents.

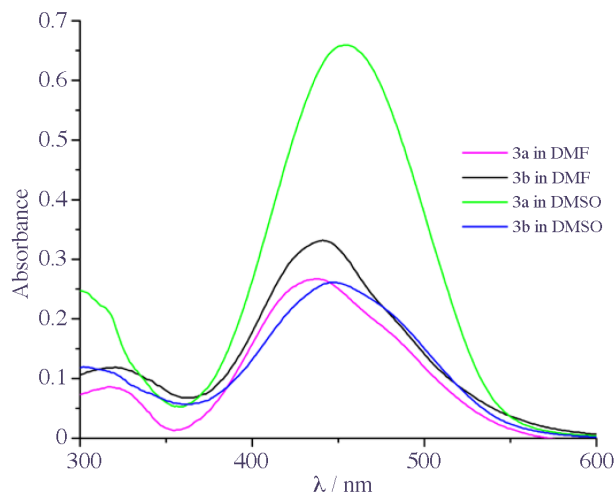


Figure 4. UV-Vis spectra of **3a** and **3b** in DMF and DMSO.

spectra of **3a** in ethanol and acid/basic solution are presented in Figure 5. It can be observed that the addition of concentrated hydrochloric acid has a small hypsochromic shift and a change in shape, indicating that the dye is not completely in the hydrazone form. On the other hand, the addition of a potassium hydroxide solution leads to deprotonation and the formation of anion/hydrazone equilibrium. Higher base quantities do not shift the equilibrium completely to the anion form, which indicates the high stability of the hydrazone form. UV-Vis maxima of anionic forms are at higher wavelengths in comparison to UV-Vis maxima of the hydrazone form, as published before.^{36–38}

Table 1. Summary of the UV–Vis absorption bands for the synthesized dyes.

| Solvent \ compound | λ_{\max} , nm ($\log \varepsilon^a$) | | Hydrazone:anion ratio | |
|--------------------|--|--------------------------------|-----------------------|-----------|
| | 3a | 3b | 3a | 3b |
| Methanol | 449 (4.39) | 446 (4.60) | 1:0 | 1:0 |
| Ethanol | 452 (4.68) | 461 (4.64) | 1:0 | 1:0 |
| i-Propanol | 438 (4.30), 457 (sh) (4.28) | 434 (4.28), 460 (sh) (4.23) | 0.56:0.44 | 0.33:0.67 |
| i-Butanol | 455 (4.27) | 449 (4.88) | 1:0 | 1:0 |
| Cyclohexanol | 455 (3.75) | 468 (4.54) | 1:0 | 1:0 |
| Dioxane | 457 (4.51) | 463 (4.60) | 1:0 | 1:0 |
| Methylene chloride | 442 (4.19) | 468 (4.49) | 1:0 | 1:0 |
| THF | 456 (4.72) | 462 (4.47) | 1:0 | 1:0 |
| Acetone | 454 (4.65) | 460 (4.62) | 1:0 | 1:0 |
| Acetonitrile | 452 (4.69) | 460 (4.47) | 1:0 | 1:0 |
| Acetic acid | 445 (4.76) | 451 (4.76) | 1:0 | 1:0 |
| DMF | 438 (4.43), 473 (sh) (4.29) | 439 (4.52), 477 (sh) (4.33) | 0.61:0.39 | 0.64:0.36 |
| DMSO | 455 (4.82) | 447 (4.42), 474 (sh) (4.35) | 1:0 | 0.96:0.04 |

^a ε , $\text{dm}^3 \text{mol}^{-1} \text{cm}^{-1}$.

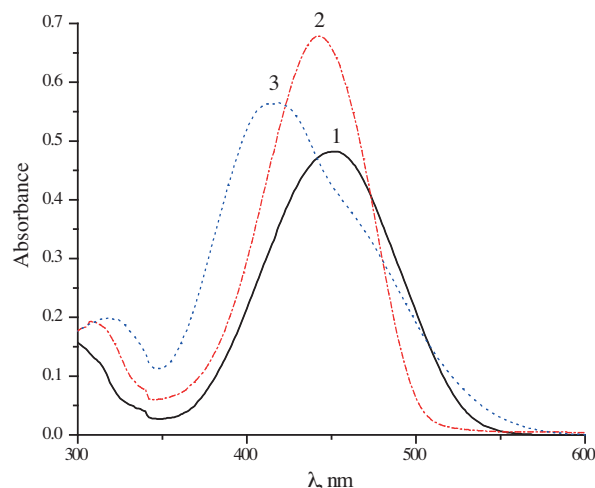


Figure 5. UV-Vis spectra of **3a** in ethanol at different pH values (1- pure ethanol; 2- with the addition of 1 drop of HCl; 3- with the addition of 1 drop of KOH).

2.2. Biological activity of the investigated aryl azo pyridone dyes

2.2.1. Biocompatibility

As a preliminary biocompatibility test, the MTT⁴⁰ test was used to reveal the new synthesized dyes' biocompatibility. The effect of the synthesized dyes on the viability of MRC-5 cells during 24 h was measured. The

results from biocompatibility analysis show a very good biocompatibility of the tested dyes in concentrations of 0.01, 0.1, 1, and 10 μM while the viability of MRC-5 cells in the presence of examined dyes was around 100%. The color of the dye solution at concentrations higher than 10 μM was not adequate for performing the color MTT assay that was used in this investigation. This is because there are no results about biocompatibility at higher concentrations. The present biocompatibility analysis clearly demonstrated the nontoxic effect of the investigated dyes on the normal human fibroblast cell line in the concentration range from 0.01 to 10 μM , qualifying them as suitable compounds for potential application in the treatment of some pathological conditions in humans.

2.3. Antiproliferative activity

According to the good biocompatibility of the investigated dyes and the potential for anticancer activity of compounds with similar structure shown in literature,⁴¹ the antiproliferative activity of the investigated dyes against cancer cell lines HCT-116 and MDA-MB-231 has been tested.⁴⁰

The assessment of the *in vitro* antiproliferative activity of the dyes against the human breast cancer MD-MB-231 cell line was performed, and the results are presented in Figure 6. It can be noticed that both dyes expressed antiproliferative activities against MD-MB-231 cells. Dye **3b** exhibited greater potential for inhibition of MD-MB-231 cell proliferation compared to dye **3a**, which expressed antiproliferative activity only at higher concentrations (10 and 1 μM). The influence of dye structure on proliferative activity was observed.

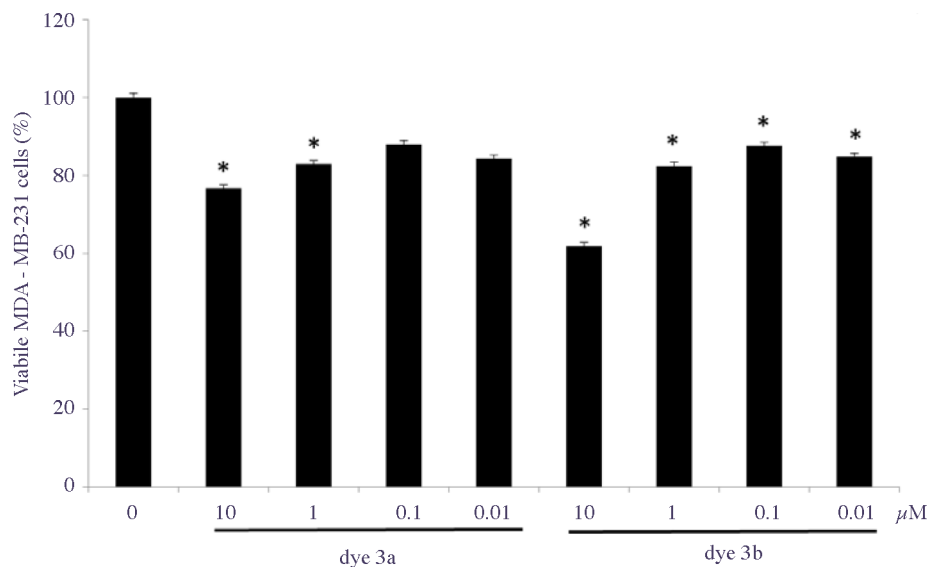


Figure 6. The effect of the investigated dyes at concentrations of 0.01, 0.1, 1, and 10 μM on the inhibition of proliferation of MDA-MB-231 cells (* $P < 0.05$ vs. control nontreated cells).

Furthermore, the noted antiproliferative activity of the dyes against the human breast cancer MD-MB-231 cell line was checked against another cell line, colon cancer HCT-116, and these results are presented in Figure 7. The antiproliferative activities of dyes against those cells were not as satisfactory as the detected activities against the MD-MB-231 cells. Both dyes exhibited slight potential for inhibition of HCT-116 cell proliferation at lower concentrations (0.1 and 0.01 μM). These results indicate that the antiproliferative activity of the investigated dyes was determined by the type of tumor cells.

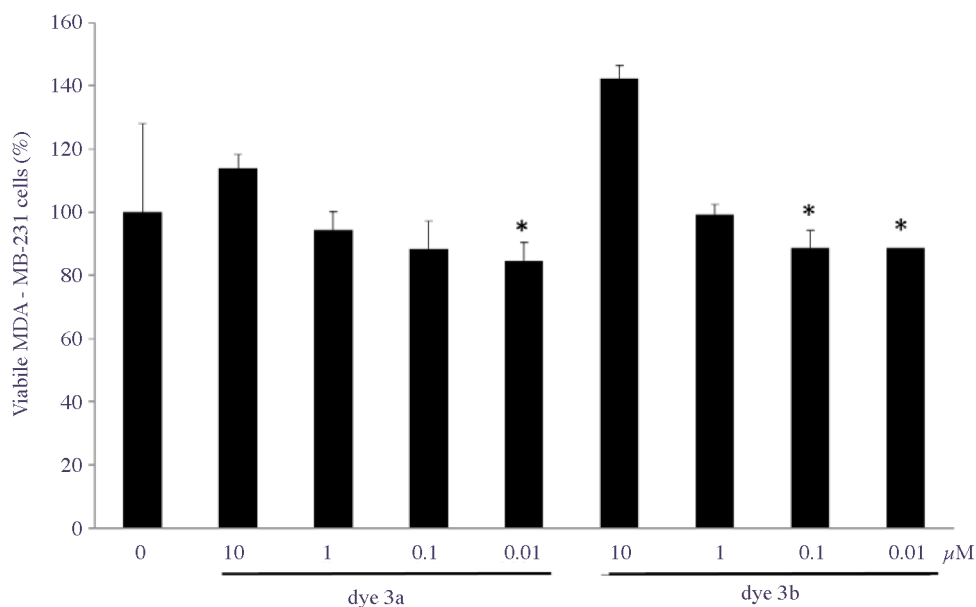


Figure 7. The effect of the investigated dyes at concentrations of 0.01, 0.1, 1, and 10 μM on the inhibition of proliferation of HCT-116 cells (* $P < 0.05$ vs. control nontreated cells).

2.4. ADMET factor profiling

One of the most important factors in the design of biologically therapeutic species is their oral bioavailability. In order to determine which of the investigated compounds possess pharmacokinetic activity, their structural properties have been tested by the empirical ‘rule of five’ established by Lipinski.⁴² The rule states that most ‘drug-like’ molecules have to satisfy the following four structural features: molecular weight lower than 500; a maximum of 5 atoms that are proton-donors of the hydrogen bonds ($-\text{OH}$ and $-\text{NH}$); a maximum of 10 atoms (N and O) that are hydrogen bond acceptors; and a calculated value of the logarithm of the octanol–water partition coefficient ($\log P$) lower than 5. Molecules satisfying these rules may potentially exhibit good in vivo permeability.⁴³ Additional structural features that have to be considered in attempts to propose a corresponding SAR model of investigated molecules are number of rotatable bonds lower than 8 and low polar surface area ($<140 \text{ \AA}^2$).

In accordance with the biological data and ADMET profiling, **3b** has been highlighted as a promising antiproliferative agent against MD-MB-231 cells (Table 2). The main difference between **3a** and **3b** is in the log P -value, which seems to be crucial for the determination of the biological activity. Therefore, further studies have to be directed towards the synthesis of novel **3b** derivatives, which may potentially exhibit excellent biological activities against different cancer cells.

3. Experimental

3.1. Materials and methods

All chemical reagents were obtained commercially from Aldrich (USA), Fluka (Germany), Fischer (USA), and Merck (Germany) and were used without any further purification. The melting points were determined in capillary tubes using a Stuart SMP30 melting point system (UK). The IR spectra were obtained using a Bomem MB-Series 100 Fourier transform-infrared (FT-IR) spectrophotometer (USA) in the form of KBr pellets. The

Table 2. Evaluation of drug candidates. All parameters are obtained from the program Molinspiration Cheminformatics 2017.

| No. | Molecular weigh | miLog P | Hydrogen bonds | | Rotatable bonds | Topological polar surface area/Å ² |
|----------------|-----------------|---------|---------------------|------------------------|-----------------|---|
| | | | Donors ^a | Acceptors ^b | | |
| 3a | 370.37 | 3.11 | 3 | 8 | 3 | 126.80 |
| 3b | 432.44 | 4.46 | 3 | 8 | 4 | 126.80 |
| Ideal compound | < 500 | < 5 | < 5 | < 10 | < 8 | < 140 |

^a A donor indicates any O–H or N–H group.

^b An acceptor indicates any O or N, including those in donor groups.

¹H and ¹³C spectra were taken on a Varian Gemini 2000 (USA; 200 Hz and 50 Hz, respectively) in deuterated dimethyl sulfoxide (DMSO-*d*₆) with tetramethylsilane (TMS) as an internal standard at room temperature (25 °C). Elemental analysis was performed using a Vario EL III elemental analyzer (Germany). The ultraviolet-visible (UV-Vis) absorption spectra were recorded on a Shimadzu 1700 spectrophotometer (Japan) in the region of 300–600 nm at a concentration 1×10^{-5} mol dm⁻³. The obtained dyes were analyzed by use of a high-performance liquid chromatograph (Surveyor, Thermo Fisher Scientific, USA) coupled to a linear ion trap mass spectrometer (LTQ XL, Thermo Fisher Scientific, USA). The flow rate of the mobile phase was 0.3 mL min⁻¹, and the mobile phase contained 40% water, 50% methanol, and 10% formic acid (0.1%). Mass spectra and MS² spectra were obtained by the use of electrospray ionization in the positive ionization mode.

3.2. Synthesis

3.2.1. Synthesis of 4-(1*H*-benzo[d]imidazol-2-yl)aniline (1)

4-(1*H*-Benzo[d]imidazol-2-yl)aniline was synthesized from *o*-phenylenediamine and *p*-aminobenzoic acid in the presence of an acid as a dehydrating agent.^{31,32}

A mixture of *o*-phenylenediamine (30 mmol) and *p*-aminobenzoic acid (45 mmol) was refluxed in *o*-phosphoric acid (30 mL) at 180–200 °C for 4 h on an oil bath. After that, the reaction mixture was cooled to 50–60 °C and poured onto crushed ice. The reaction mixture was then neutralized with a sodium hydroxide solution (10%, 70 mL) and the precipitate was collected by filtration. The raw product was washed with an excess 10% sodium hydroxide solution and water and then dried. The product was further purified by crystallization from ethanol. Mp: 248.1–249.8 °C (lit. mp: 248 °C⁴⁴; yield = 55%; IR (KBr) ν_{max} /cm⁻¹: 3438 (NH benzimidazole), 3360, 3216 (NH₂ aminophenyl), 3050 (CH arom), 1621 (C=N), 1605 (C=C arom). ¹H NMR (DMSO-*d*₆) δ /ppm: 5.66 (2H, s, NH₂ aminophenyl), 6.73 (2H, d, *J* = 8 Hz, Ar), 7.14–7.20 (2H, m, Ar), 7.51–7.58 (2H, m, Ar), 7.91 (2H, d, *J* = 8 Hz, Ar), 12.42 (1H, brs, NH benzimidazole).

3.2.2. Synthesis of 2-pyridones

2-Pyridones were prepared according to literature procedures^{33,34} from an ester and cyanoacetamides.

6-Hydroxy-4-methyl-2-oxo-1,2-dihydropyridine-3-carbonitrile (2a)

A mixture of ethyl acetoacetate (0.012 mol), cyanoacetamide (0.019 mol), and potassium hydroxide (0.014 mol) in methanol (20 mL) was mixed and heated under reflux for 1 h. The reaction mixture was cooled and filtrated.

The obtained crystals were dissolved in hot water and filtrated, and after cooling to room temperature, the solution was acidified with hydrochloric acid. The formed crystals were isolated by filtration, then washed with water and methanol. The product was further purified by crystallization from acetone. Mp: 315.1–316.2 °C (lit. mp: 315–316 °C;³⁵ yield = 50%; IR (KBr) ν_{max}/cm^{-1} : 3420 (OH), 3367 (NH), 2224 (CN), 1603 (C = O). ¹H NMR (DMSO-*d*₆) δ/ppm : 2.23 (3H, s, CH₃), 5.59 (1H, s, Ar).

3.2.2.2. 6-Hydroxy-2-oxo-4-phenyl-1,2-dihydropyridine-3-carbonitrile (2b)

A mixture of ethyl benzoylacetate (10 mmol), cyanoacetamide (10 mmol), and potassium hydroxide (10 mmol) was heated under reflux in ethanol (10 mL) for 20 h. After cooling to room temperature, the product was isolated by filtration and then purified by crystallization from ethanol. Mp: 279.1–280.0 °C (lit. mp: 280 °C);⁴⁵ yield = 55%; IR (KBr) ν_{max}/cm^{-1} : 3418 (OH), 3320 (NH), 2227 (CN), 1653 (C=O); ¹H NMR (DMSO-*d*₆) δ/ppm : 6.27 (1H, s, Pyr); 7.40–7.61 (5H, m, Ar); 11.73 (1H, s, OH).

3.2.3. Synthesis of dyes

Both azo compounds were synthesized according to the procedure described as published before³⁵ starting from 4-(1H-benzo[d]imidazol-2-yl)aniline. The products were purified by crystallization from *N,N*-dimethyl formamide. Both dyes were obtained as dark red solids.

General procedure: The corresponding 2-pyridone (3 mmol) was first dissolved in 4 mL of sodium hydroxide solution (3 mmol) and then cooled to 0–5 °C. A diazonium solution was prepared by the addition of a sodium nitrate solution (3.3 mmol) in water (1.5 mL) to a solution of 4-(1H-benzo[d]imidazol-2-yl)aniline (3 mmol) in conc. hydrochloric acid (1.1 mL) cooled to 0–5 °C. The 2-pyridone solution was then slowly added to the cold diazonium solution for 10 min and stirred at 0–5 °C for 4 h. The formed solid was isolated by filtration, washed with ethanol, and then dried (Figure 1).

3.2.3.1. 5-((4-(1H-Benzo[d]imidazol-2-yl)phenyl)diazonyl)-6-hydroxy-4-methyl-2-oxo-1,2-dihydropyridine-3-carbonitrile (3a)

Yield: 41%; mp > 330 °C; FT-IR (KBr, ν_{max}/cm^{-1}): 3426 (NH on hydrazone form), 2222 (CN), 1655, 1640 (C=O on heterocyclic); ¹H NMR (DMSO-*d*₆) δ/ppm : 2.61 (3H, s, CH₃), 7.25–7.32 (2H, m, Ar-H), 7.63–7.72 (2H, m, Ar-H), 7.89 (2H, d, *J* = 8.8 Hz, Ar-H), 8.32 (2H, d, *J* = 8.8 Hz, Ar-H), 12.15 (1H, s, NH pyridone), 13.05 (1H, s, NH imidazole), 14.71 (1H, s, NH hydrazone); ¹³C NMR (50 MHz, DMSO-*d*₆) δ/ppm : 17.0 (Me), 101.6 (Py), 115.4 (CN), 118.1 (Ar), 122.8 (Ar), 124.7 (Py), 126.8 (Ar), 128.3 (Ar), 130.5 (Ar), 143.0 (Ar), 151.9 (Ar), 160.7 (Py), 161.2 (Py), 161.9 (Py); Anal. Calcd for C₂₀H₁₄N₆O₂ (370.12): C, 64.86; H, 3.81; N, 22.69. Found: C, 64.05; H, 3.79; N, 22.21. ESI-MS (*m/z*, positive mode) = 371.10 (molecular ion peak), 209.10 (base ion peak).

3.2.3.2. 5-((4-(1H-Benzo[d]imidazol-2-yl)phenyl)diazonyl)-6-hydroxy-2-oxo-4-phenyl-1,2-dihydropyridine-3-carbonitrile (3b)

Yield: 45%; mp 300.7–301.5 °C; FT-IR (KBr, ν_{max}/cm^{-1}): 3424 (NH on hydrazone form), 2225 (CN), 1639, 1619 (C=O on heterocyclic); ¹H NMR (DMSO-*d*₆) δ/ppm : 7.18–7.26 (2H, m, Ar-H), 7.48–7.70 (7H, m, Ar-H), 7.38 (2H, d, *J* = 8 Hz, Ar-H), 8.12 (2H, d, *J* = 10 Hz, Ar-H), 12.03 (1H, s, NH pyridone), 12.99 (1H, s, NH

imidazole), 14.55 (1H, s, NH hydrazone); ^{13}C NMR (DMSO- d_6) δ /ppm: 101.1 (Py), 115.2 (Ar), 115.4 (CN), 117.6 (Ar), 123.0 (Ar), 124.5 (Py), 127.2 (Ar), 128.1 (Ar), 129.8 (Ar), 130.3 (Ar), 133.0 (Ar), 138.7 (Ar), 142.7 (Ar), 150.3 (Ar), 160.9 (Py), 161.2 (Py), 161.8 (Py); Anal. Calcd for $\text{C}_{25}\text{H}_{16}\text{N}_6\text{O}_2$ (432.13): C, 69.44; H, 3.73; N, 19.43. Found: C, 68.25; H, 3.65; N, 18.95. ESI-MS (m/z , positive mode) = 433.20 (molecular ion peak), 209.10 (base ion peak).

3.3. Biological evaluation

3.3.1. Compounds and solutions

MTT was dissolved (5 mg cm^{-3}) in phosphate-buffered saline (pH 7.2) and filtered ($0.22\ \mu\text{m}$) before use. RPMI 1640 cell culture medium, fetal bovine serum (FBS), and MTT were purchased from Sigma Chemical Company (USA).

3.3.2. Cell lines

Normal human fibroblast (MRC-5), human colon cancer (HCT-116), and human breast cancer (MDA-MB-231) cell lines were maintained in monolayer cultures using nutrient medium RPMI 1640 with 10% FBS and antibiotics.

3.3.3. Biocompatibility assay

The biocompatibility testing of newly synthesized compounds is the first step in their biological characterization. The normal human fibroblast cell line (MRC-5) was used for the evaluation of biocompatibility. MRC-5 cells were seeded in 96-well microtiter plate and cultivated in full culture media for 24 h. After that, the investigated compound was added to cells in final concentrations of 0.01, 0.1, 1, 10, and $100\ \mu\text{M}$, except in the control wells, where only the medium was added. Thus, prepared cell cultures were incubated for an additional 24 h. At the end of this period, the MTT test,⁴⁶ as modified by Ohno and Abe,⁴⁰ was used for measuring the cell viability/proliferation.

3.4. Treatment of cell lines for antiproliferative in vitro screening

The target cell lines HCT-116 and MDA-MB-231 were seeded in quadruplicates into 96-well, flat-bottomed microtiter plates in 0.1 cm^3 of culture medium. After cell adaptation and the adherence of both cell lines, 0.1 cm^3 of the investigated compound was added to cells in final concentrations of 0.01, 0.1, 1, 10, and $100\ \mu\text{M}$, except in the control wells, where only the medium was added to the cells and was incubated for an additional 24 h. The effect of the investigated compounds on cell survival was determined at the end of the incubation period by the MTT test⁴⁰ as described in the previous paragraph. The antiproliferative effect of the compounds was expressed as a percentage of viable cells.

Acknowledgment

This work was financially supported by Ministry of Education, Science, and Technological Development, Republic of Serbia, under Grants No. 172013 and 173052.

References

1. Salahuddin; Shaharyar, M.; Mazumder, A. *Arab. J. Chem.* **2017**, *10*, S157-S173.
2. Neidle, S. *Principles of Nucleic Acid Structure*; Academic Press: Amsterdam, the Netherlands, 2008.
3. Zhu, W.; Da, Y.; Wu, D.; Zheng, H.; Zhu, L.; Wang, L.; Yan, Y.; Chen, Z. *Bioorg. Med. Chem.* **2014**, *22*, 2294-2302.
4. Zhan, P.; Li, D.; Li, J.; Chen, X.; Liu, X. *Mini Rev. Org. Chem.* **2012**, *9*, 397-410.
5. Piras, S.; Loriga, M.; Paglietti, G.; Sparatore, F.; Demontis, M. P.; Varoni, M. V.; Fattaccio, M. C.; Anania, V. *Farmaco* **1993**, *48*, 1249-1259.
6. Brahmeshwari, G.; Gullapelli, K. *Int. J. Chem. Sci.* **2014**, *12*, 885-893.
7. Gullapelli, K.; Thupurani, M. K.; Brahmeshwari, G. *Int. J. Pharma Bio Sci.* **2014**, *5*, 682-690.
8. Dutta Gupta, S.; Revathi, B.; Mazaira, G. I.; Galigniana, M. D.; Subrahmanyam, C. V. S.; Gowrishankar, N. L.; Raghavendra, N. M. *Bioorg. Chem.* **2015**, *59*, 97-105.
9. Vinayak, G. R.; Sachin, V. V.; Vasudev, J. S. *Inventi Impact Med Chem* **2012**, *2012*, 170-172.
10. Verma, N.; Singh, R. B.; Srivastava, S.; Dubey, P. *J. Chem. Pharm. Res.* **2016**, *8*, 365-374.
11. Ajani, O. O.; Aderohunmu, D. V.; Ikpo, C. O.; Adedapo, A. E.; Olanrewaju, I. O. *Arch. Pharm. (Weinheim)* **2016**, *349*, 475-506.
12. Arulmurugan, S.; Kavitha, H. P.; Sathishkumar, S.; Arulmozhi, R. *Mini Rev. Org. Chem* **2015**, *12*, 178-195.
13. Soni, B. *PharmaTutor Magazine* **2014**, *2*, 110-118.
14. Enumula, S.; Pangal, A.; Gazge, M.; Shaikh, J. A.; Ahmed, K. *Res. J. Chem. Sci.* **2014**, *4*, 78-88.
15. Gaba, M.; Singh, S.; Mohan, C. *Eur. J. Med. Chem.* **2014**, *76*, 494-505.
16. El Rashedy, A. A.; Aboul-Enein, H. Y. *Curr. Drug Ther.* **2013**, *8*, 1-14.
17. Vučijak, N. Ž.; Petrović, S. D.; Bezbradica, D. I.; Knežević-Jugović, Z. D.; Mijin, D. Ž. *Hem. Ind.* **2009**, *63*, 353-360.
18. Abdel-Aziz, A.; El-Subbagh, H.; Kunieda, T. *Bioorg. Med. Chem.* **2005**, *13*, 4929-4935.
19. Fan, X.; Feng, D.; Qu, Y.; Zhang, X.; Wang, J.; Loiseau, P. M.; Andrei, G.; Snoeck, R.; De Clercq, E. *Bioorg. Med. Chem. Lett.* **2010**, *20*, 809-813.
20. Chen, W.; Zhan, P.; Rai, D.; De Clercq, E.; Pannecouque, C.; Balzarini, J.; Zhou, Z.; Liu, H.; Liu, X. *Bioorg. Med. Chem.* **2014**, *22*, 1863-1872.
21. Thompson, P.; Manganiello, V.; Degerman, E. *Curr. Top. Med. Chem.* **2007**, *7*, 421-436.
22. Mirković, J. M.; Mijin, D. Ž.; Petrović, S. D. *Hem. Ind.* **2013**, *67*, 17-25.
23. Hernández, F.; Sánchez, A.; Rendón-Vallejo, P.; Millán-Pacheco, C.; Alcaraz, Y.; Delgado, F.; Vázquez, M. A.; Estrada-Soto, S. *Eur. J. Med. Chem.* **2013**, *70*, 669-676.
24. Desai, N. C.; Shihory, N. R.; Kotadiya, G. M. *Chin. Chem. Lett.* **2014**, *25*, 305-307.
25. Mijin, D. Ž.; Ušćumlić, G. S.; Valentić, N. V. In Mondal M. I. H., Ed. *Textiles: History, Properties and Performance and Applications*; Nova Publishers: New York, NY, USA, 2014, pp. 157-186.
26. Shawali, A. S.; Zayed, M. E. M. *Turk. J. Chem.* **2013**, *37*, 413-421.
27. Desai, V. A.; Shah, M. J.; Desai, T. R.; Desai, K. R. *J. Inst. Chem.* **1996**, *68*, 58-59.
28. Savarino, P.; Viscardi, G.; Barni, E.; Carpignano, R. *Dyes Pigm.* **1988**, *9*, 295-304.
29. Mirković, J. M.; Božić, B. Đ.; Ušćumlić, G. S.; Mijin, D. Ž. In Wythers, M. C., Ed. *Advances in Materials Science Research, Vol. 26*; Nova Science Publishers: New York, NY, USA, 2016, pp. 209-253.

30. Dikshit, D. V.; Deval, S. D.; Deodhar, K. D. *Dyes Pigm.* **1985**, *6*, 39-46.
31. Khattab, M.; Galal, S. A.; Ragab, F. A. F.; El Diwani, H. I. *Res. Chem. Intermed.* **2013**, *39*, 2917-2923.
32. Khattab, M. K.; Ragab, F. A. F.; Galal, S. A.; El Diwani, H. I. *Int. J. Res. Pharm. Chem.* **2012**, *2*, 937-946.
33. Mijin, D. Ž.; Ušćumlić, G. S.; Valentić, N. V. *J. Serb. Chem. Soc.* **2001**, *66*, 507-516.
34. Alimmari, A.; Mijin, D.; Vukićević, R.; Božić, B.; Valentić, N.; Vitnik, V.; Vitnik, Ž.; Ušćumlić, G. *Chem. Cent. J.* **2012**, *6*, 1-8.
35. Dostanic, J. M.; Loncarevic, D. R.; Bankovic, P. T.; Cvetkovic, O. G.; Jovanovic, D. M.; Mijin, D. Z. *J. Environ. Sci. Heal. A* **2011**, *46*, 70-79.
36. Peng, Q.; Li, M.; Gao, K.; Cheng, L. *Dyes Pigm.* **1991**, *15*, 263-274.
37. Peng, Q.; Li, M.; Gao, K.; Cheng, L. *Dyes Pigm.* **1992**, *18*, 271-286.
38. Ertan, N.; Eyduran, F. *Dyes Pigm.* **1995**, *27*, 313-320.
39. Vitnik, V. D.; Vitnik, Z. J.; Bozic, B. D.; Valentic, N. V.; Dilber, S. P.; Mijin, D. Z.; Uscumlic, G. S. *Color. Technol.* **2017**, *133*, 223-233.
40. Ohno, M.; Abe, T. *J. Immunol. Methods* **1991**, *145*, 199-203.
41. Rezaei-Seresht, E.; Mireskandari, E.; Kheirabadi, M.; Cheshomi, H.; Rezaei-Seresht, H.; Aldaghi, L. S. *Chem. Pap.* **2017**, *71*, 1463-1469.
42. Lipinski, C.A.; Lombardo, F.; Dominy, B.W.; Feeney, P.J. *Adv. Drug Deliv. Rev.* **1997**, *23*, 3-25.
43. Remko, M.; Swary, M.; Bickelhaupt, F. M. *Bioorg. Med. Chem.* **2006**, *14*, 1715-1728.
44. Shingalapur, R. V. ; Hosamani, K. M. *Catal. Lett.* **2010**, *137*, 63-68.
45. Roch, J.; Müller, E.; Narr, B.; Nickl, J.; Haarmann, W. US Patent 4260621, 1981.
46. Mosmann, T. *J. Immunol. Methods* **1983**, *65*, 55-63.